NASA Technical Memorandum 106969

Characterization of Cobalt-Dipped Nickel Electrodes With Fibrex Substrates

Carolyn A. Youngman and Margaret A. Reid
Lewis Research Center
Cleveland, Ohio

August 1995

National Aeronautics and
Space Administration

CHARACTERIZATION OF COBALT-DIPPED NICKEL ELECTRODES WITH FIBREX SUBSTRATES

Carolyn A. Youngman and Margaret A. Reid
National Aeronautics and Space Administration
Lewis Research Center
Cleveland, Ohio 44135

SUMMARY

Nickel electrodes using fibrous substrates have poorer initial utilization of the active material than those using conventional nickel sinter substrates. Previous investigators had shown that utilization can be dramatically improved by dipping these electrodes in a cobalt solution immediately after the electrochemical impregnation, before formation and cycling is carried out. The present study looked at the gas evolution behavior of dipped and undipped electrodes, impedance curves, and the charge-discharge curves to try to understand the reasons for the improvement in utilization. Impedance measurements under open circuit conditions indicate that some of the improvement is due to a reduction in the ohmic resistance of the surface layer of the particles, in agreement with earlier work. The charge-discharge curves suggest that there may also be an additional increase in the ohmic resistance of the surface layer of the undipped electrode during charging.

INTRODUCTION

The use of lightweight fibrous materials as substrates for nickel electrodes in nickel-hydrogen and other nickel batteries has met with limited success in the past. Replacement of the heavier and more expensive nickel sinter substrate continues to be of interest, especially for use in space applications where low weight and high energy density, together with long cycle life, is a primary goal. These electrodes can potentially give much higher energy density, even when nickel fibers are used, because substrates with much higher porosity than the standard 80 to 82 percent porosity sintered nickel electrodes allow a higher level of impregnation (refs.1 and 2). Previous work has shown that these fibrous electrodes cannot be impregnated by the usual conditions for sintered electrodes, but adequate loading can be achieved if the current densities and times are modified for each individual fiber type and porosity (ref. 3). However, even when the proper loading is achieved, the utilization of these electrodes is very poor for at least the first few hundred cycles, and thus the theoretical energy density cannot be achieved. The initial utilization must be able to be increased if the actual energy density of these lightweight electrodes is to be superior to that of the standard sintered electrodes.

It has been found that dipping the newly impregnated electrodes in a solution of cobalt nitrate can markedly improve the initial utilization (refs. 4 to 6). In the present study, this phenomena was investigated by studying the oxygen evolution of both dipped and undipped electrodes, impedances, and the charge-discharge curves.

EXPERIMENTAL PROCEDURES

Impregnation and Formation

The substrate used in this investigation was Fibrex, available from National Standard Company. This material is available with different fiber diameters, porosities, and thicknesses. It can also be made with nickel and/or cobalt powder incorporated into the electrode in various proportions. The material used here had a fiber diameter of 20 μm, 85 percent porosity, and a thickness of 40 mil. The ratio of nickel fiber to metal powder was 80:20, and 15 percent of the metal powder was cobalt.

In order to compare the dipped and undipped electrodes on an equal basis and to eliminate concerns that differences in the behavior might be due to differences in impregnation procedure or loading level, samples of Fibrex plaque were impregnated and then cut in half. One half was then dipped in the cobalt solution. The two halves were then compared.

Nickel leads were spot welded to each side of a 6.35- by 7.62-cm (2.5- by 3-in.) piece of unimpregnated Fibrex. It was then passivated in a hot water bath at 40 °C for 20 min and then dried at 350 °C for 20 min. After the substrate was weighed, it was impregnated in an aqueous bath containing 1.5 M $Ni(NO_3)$, 0.175 M $Co(NO_3)$ and 0.075 M $NaNO_3$ at a pH of 3.0 to 3.5 and temperature of 95 °C. The pH was maintained with 1:1 HNO_3, and the solution level was maintained by additions of warm impregnation solution. The solution was stirred continuously. A counter electrode of nickel sheet was held on each side of the working electrode at a fixed position in order to maintain a uniform current density over the surface of the electrode. For this particular Fibrex structure, it has been found that the desired impregnation level of 1.6 g/cm^3 void can
be achieved with a current density of 77.5 mA/cm^2 (0.5 A/in.^{2}) for 4 hr. (The loading level is very sensitive to changes in the Fibrex structure, and the exact impregnation conditions have to be worked out for each structure).

After impregnation, the electrode was divided into two equal pieces, and one half was soaked in a solution of 1.8 M $Co(NO_3)_2$ for 20 min at room temperature, whereas the other remained untreated.

The electrodes were formed by charging for 16 to18 hr at a C/10 rate and discharging at a rate of C/4 in 26 percent KOH to a limit of -0.20 V versus a Hg/HgO reference electrode. The initial rates were based on the theoretical capacity determined by the weight gain during impregnation. Two formation cycles were performed on the electrodes used for the oxygen evolution measurements and three on the electrodes used for the impedance and charge-discharge curves so that the electrodes were partially conditioned, but not enough to eliminate the differences between the electrodes at the early stages of cycling. The electrodes were then rinsed and dried in an oven for 4 to 5 hr at 60 °C, to determine the final loading level since there is a loss of some material during the formation procedure.

The Hg/HgO reference electrode was constructed from heat-shrink tubing about 4 mm in diameter and from 10 to 20 cm long (The length the electrode is made depends on where it will be used.). A small plug of separator material (4 to 5 mm long) is forced into one end of the tube and the tube is shrunk enough to hold the plug in but not enough to close the tube. A small amount of Hg and HgO is inserted into the tube and a thin Pt lead wire is inserted. Before insertion, a short length of small diameter heat shrink tubing is sealed around the portion of the Pt wire where the Pt wire exits the outer tube. The outer tube is then shrunk around the Pt wire. The inner heat shrink tubing holds the Pt wire in position so that it will maintain contact with the Hg/HgO. The electrode is placed into a jar containing the KOH electrolyte at least overnight to allow the electrolyte to wick into the tube. It is important to keep the reference electrode in the same percent solution of electolyte in a tightly closed container when not in use. Contamination by carbon dioxide can change the concentration of the electrolyte in the reference electrode over time, which will change its potential. The voltages of these electrodes should be checked periodically against a calomel electrode or a fresh Hg/HgO electrode. Since the ohmic resistance within the electrode will vary depending on the solution resistance through the plug of separator material, impedance and charge-discharge curves were made by using the same reference electrode.

This type of construction is useful for small containers, particularly for positioning the electrode with respect to working electrodes, thus a reproducible internal resistance (IR) can be obtained between the reference and the working electrode.

Oxygen Evolution Measurements

Oxygen evolution, impedance and charge-discharge measurements were made on a number of electrodes. The measurements of oxygen evolution were made on an electrode pair that had the optimum loading of about 1.60 g/cc void. The theoretical capacity of each half of this electrode after the two formation cycles was 0.88 Ah.

After formation, the pair of electrodes were cycled five times at a charge rate of C/4 plus 50 percent overcharge and discharged at a rate of C/2 to -0.20 V versus a Hg/HgO reference electrode. The electrodes were placed in a large glass dish containing 500 ml of 26 percent KOH and connected in series to a power supply and an Ah meter. An inverted funnel attached by rubber tubing to an inverted 100 ml buret was placed over each electrode, and the buret was evacuated so as to fill it with electrolyte. During the charging, the oxygen displaced the electrolyte in the buret. The volume of oxygen evolved was recorded as a function of the Ah of charge. The charging was interrupted at intervals to allow the very tiny oxygen bubbles to rise to the surface of the buret, and the buret was lightly tapped so that bubbles would not adhere to the sides of the buret. The counter electrode was a strip of nickel placed around the sides of the glass container so that the hydrogen generated from this electrode during the experiment would not enter the burets and interfere with the measurement of the oxygen evolution. The apparatus is shown in figure 1.

In this cell, the reference electrode could not be placed in a reproducible position with respect to the working electrodes. The large changes in voltage at the end of discharge could be used to determine the capacity of the electrode, but the measurements could not be used to accurately compare the charge and discharge curves of the dipped and undipped electrodes because of the large and uncertain values of the IR losses attributed to solution resistance between the reference and working electrodes. A different cell with better control of the solution resistance was used for comparing the charge-discharge curves and impedance measurements as discussed in the following section.

Impedance Measurements

In order to compare the charge-discharge curves on an IR-free basis, the ohmic resistances had to be measured accurately. Impedance measurements were carried out to determine this, and also to find out whether there were any differences in the kinetic resistances at high states of charge due to differences in oxygen evolution overvoltage.

Impedance measurements and charge-discharge curves were made using a prismatic cell with spacers of plastic screen. Cutouts were made in some of the screens to position the reference, counter and working electrodes with respect to each other so as to hold them in fixed reproducible positions. Other screens were used as separators between the electrodes. The same reference electrode was used for both the dipped and undipped electrodes.

Impedances were measured using a 1250 Solartron Frequency Response Analyzer and a Solartron 1286 Electrochemical Interface with ZPlot software in a Windows environment (ZWIN). The electrodes were charged at a C/10 rate for 16 hr, then discharged to the desired voltage. Measurements were made at open-circuit voltages from 0.480 to 0.160 V versus the Hg/HgO reference electrode which covers the entire range from fully charged to fully discharged. Before each measurement, the electrode was held at the desired open-circuit voltage to equilibrate until the current fell below about 10 mA, usually for several hours.

The impedance measurements always showed a greater ohmic resistance for undipped electrodes. The data reported here were for a pair of electrode samples with a loading of 1.35 g/cc void. The dipped and undipped portions of this pair of electrodes had theoretical capacities of 0.812 and 0.708 Ah, respectively.

Charge-Discharge Curves

After the impedance measurements, the electrodes were charged for 4.4 hr at a C/4 rate and discharged at a C/2 rate to a limit of 0.00 V versus the Hg/HgO reference electrode. (The limit of 0.00 V was used for these measurements rather than the -0.20 V used in the formation and oxygen evolution measurements because of the smaller IR drop in this cell.)

A Solartron 1286 Potentiostat and CorrWin software (Scribner Associates) were used for data collection and analysis.

ANALYTICAL ANALYSIS

In order to determine whether any appreciable amount of Co had been absorbed or adsorbed by the dipping process, the electrodes were examined by AA, SEM, and EDAX. No changes in the cobalt levels were detected (i.e., only very small amounts were absorbed from the solution in which the electrodes were dipped). This result was expected, since these electrodes were made from Fibrex with a large cobalt content and also were impregnated with active material containing 10 percent Co. No changes would have been expected unless a very large amount of cobalt had been absorbed.

RESULTS AND DISCUSSION

Oxygen Evolution Experiments

Figure 2 shows the oxygen evolution for the dipped electrode as a function of number of Ah of charge for the five charge-discharge cycles. It can be seen that the oxygen evolution fell with successive charges and discharges. The data are similar for the undipped electrode, but the volumes of oxygen are larger. No measurements were taken until the first oxygen evolution was noticed, at about 0.40 Ah. Note that the Ah scale is not linear, but the bar chart representation was used to better illustrate the trends in the data. The theoretical capacity of each electrode used in the oxygen evolution experiment with a loading of 1.60 g/cc void was 0.88 Ah.

Figure 3 shows the volume of oxygen produced versus the fraction of theoretical capacity of the nickel electrode for the third charging cycle. The dipped electrode does not evolve appreciable oxygen until it is about 60 percent charged, whereas the undipped electrode starts evolving oxygen when it is about 40 percent charged. There is a good bit of scatter in the data because of the length of time that it takes for the small oxygen bubbles to rise. It was not practical to wait more than 5 to 10 min after each charge interval. Small amounts of oxygen may also have been lost through the stopcock of the buret. The data for the third cycle are shown here, since there was the best agreement between the capacity of the nickel electrode calculated from the oxygen evolution measurements and the capacity measured on discharge.

The amount of charge going toward the evolution of oxygen is calculated by correcting the volume of oxygen to standard conditions and calculating the equivalents of oxygen produced. Once this is known, the amount of charge contributing toward charging the nickel electrode is found by subtracting the amount used for oxygen

evolution from the total amount of charge. The utilization and charge efficiencies can then be determined. Sample calculations are shown in tables I and II.

The utilizations of each electrode are shown in figure 4 where utilization is defined as the fraction of the Ah contributing toward charging the nickel electrode versus the theoretical capacity. If the entire charge goes toward charging the nickel electrode, the curves would follow the 100-percent utilization line. Deviations from this line indicate the amount of charge going toward oxygen evolution. The utilization can also be calculated as the fraction of Ah withdrawn on discharge versus the theoretical capacity. There was good agreement between the utilizations determined during charge and those during discharge.

Overall charge efficiency is defined as the Ah used to charge the nickel electrode divided by the total Ah of charge input. Incremental charge efficiency is the percent of charge in an interval that contributes toward charging the nickel electrode.

TABLE I.—CALCULATION OF UTILIZATION AND CHARGE EFFICIENCY FOR UNDIPPED ELECTRODE FROM O_2 EVOLUTION MEASUREMENTS. (THIRD CYCLE, THEORETICAL CAPACITY 0.88 Ah)

Ah charge	Fraction of theoretical capacity added	Volume O_2 evolved, cc	Volume O_2 at standard temperature and pressure, cc (a)	Calculated Ah used for O_2 evolution	Ah Ni = Ah charge - Ah O_2 evolution	Utilization = Ah Ni/ theoretical capacity	Overall charge efficiency and incremental charge efficiency, percent
0.00	0.00	0.0	0.0	0.00	0.00	0.00	
0.42	0.48	0.2	0.2	0.00	0.42	0.47	100, 100
0.63	0.71	17.0	16.0	0.07	0.55	0.63	87, 64
0.84	0.95	55.3	51.9	0.248	0.59	0.67	70, 18
0.94	1.07	75.6	71.1	0.340	0.60	0.68	64, 13
1.00	1.13	86.0	80.8	0.387	0.61	0.69	61, 11
1.05	1.19	98.2	92.3	0.441	0.61	0.69	59, 0
1.10	1.25	110	104	0.497	0.60	0.69	55, -1
1.15	1.30	123	116	0.554	0.60	0.68	52, -1
1.20	1.36	133	125	0.600	0.60	0.68	50, 1
1.26	1.43	145	136	0.650	0.61	0.69	48, 5

(a) The oxygen volume was corrected for the water vapor pressure over KOH.

TABLE II.—CALCULATION OF UTILIZATION AND CHARGE EFFICIENCY FOR DIPPED ELECTRODE FROM O_2 EVOLUTION MEASUREMENTS. (THIRD CYCLE, THEORETICAL CAPACITY 0.88 Ah)

Ah charge	Fraction of theoretical capacity added	Volume O_2 evolved, cc	Volume O_2 at standard temperature and pressure, cc (a)	Calculated Ah used for O_2 evolution	Ah Ni = Ah charge - Ah O_2 evolution	Utilization = Ah Ni/ theoretical capacity	Overall charge efficiency and incremental charge efficiency, percent
0.00	0.00	0.0	0.0	0.00	0.00	0.00	
0.42	0.48	0.0	0.0	0.00	0.42	0.47	100, 100
0.63	0.71	0.6	0.56	0.00	0.63	0.71	100, 99
0.84	0.95	21.2	19.9	0.10	0.74	0.84	88, 56
0.94	1.07	40.9	38.4	0.18	0.76	0.86	81, 15
1.00	1.13	51.9	48.7	0.23	0.76	0.86	76, 6
1.05	1.19	62.5	58.8	0.28	0.77	0.87	73, 9
1.10	1.25	76.0	71.4	0.34	0.76	0.86	69, -16
1.15	1.30	86.4	81.2	0.39	0.76	0.86	66, 11
1.20	1.36	97.4	91.5	0.43	0.77	0.87	64, 5
1.26	1.43	110	103	0.49	0.76	0.87	60, -4

(a) The oxygen volume was corrected for the water vapor pressure over KOH.

It has been theorized that the greater utilization of dipped electrodes is due to formation of a more conductive film on the surface of the active material (ref. 7). It is also possible that there is a greater oxygen overpotential in the dipped electrodes causing a decrease in oxygen evolution as is suggested by the results of Haenen et al. (ref. 8). (However, other workers have seen an increase in oxygen evolution on cobalt oxide deposited on NiO (ref. 9).) Impedance measurements were performed to look at the ohmic resistances and the kinetic resistances of the electrodes to help determine the reasons for the differences.

Complex plane plots for the dipped and undipped electrodes at 0.440 V versus Hg/HgO, a potential where small amounts of oxygen are being evolved, are given in figure 5. When the electrodes were held at this voltage before the impedance measurements, the steady state currents were about 0.2 mA/cm^2.

Analysis of these types of plots is difficult and has not been carried out as yet. Curves with inductive portions such as those with loops going into the positive Z' portion of the curve are usually interpreted as indicating adsorption on the electrodes. More direct measurements such as Tafel slopes are needed in order to determine how the cobalt dip has affected the oxygen evolution potential.

Typical examples of plots at intermediate and low states of charge (0.290 and 0.220 V) are shown in figures 6 and 7. The plots at these voltages can be interpreted simplistically in terms of the simple equivalent circuit shown in figure 8 (ref. 10). Note that the scale of the plots increases as the voltage is lowered.

The ohmic resistances, except at the very highest potentials, average about 6.51 mΩ for the dipped electrode and 9.05 mΩ for the undipped electrode. It is clear that the cobalt has reduced the ohmic resistance, and since the solution resistance could not be affected, this must be due to the formation of a more conductive surface film on the active material as theorized by Oshitani, et al. (ref. 7).

The kinetic resistances in the undippped electrode are also larger than for the dipped electrode, although there is a lot of scatter in the data for the undipped electrode. The increased kinetic resistances are probably due to the fact that, after the few cycles have taken place, there is a smaller proportion of *active* material in the undipped electrode than in the dipped electrode. This may affect the rate of proton diffusion through the active material and thus the rate of electrode reactions.

Figures 9 and 10 are the charge and discharge curves for the two electrodes uncorrected for IR losses, whereas figures 11 and 12 are corrected for IR losses. In the latter figures, the voltages are plotted against state of charge (determined using the experimental discharge capacities rather than the theoretical capacities). The capacities of the dipped and undipped electrodes (the same electrodes were used for the impedance measurements with a loading of 1.35 g/cc void) at this point are 0.584 and 0.447 Ah, respectively. Comparing this against the theoretical capacities of 0.812 and 0.708 Ah gives utilizations of 72 and 63 percent, respectively.

Correcting for the IR losses and expressing the data in terms of the state of charge reveals that the discharge curves for the dipped and undipped curves are very similar, but the charging voltages for the undipped electrode are still considerably higher. Thus the differences cannot be ascribed completely to the differences in ohmic resistance. The difference in voltage is about the same over the whole state of charge, not just at the higher voltages where oxygen is being evolved. Whether this is due to an increase in the ohmic resistance of the surface film during charging or whether it is due to changes in oxygen overvoltage is unclear and needs further experimental analyses.

Experiments on Other Electrodes

Cobalt dipping was performed on various electrodes that had been cycled extensively to determine whether performance could be improved, but no improvement was noted. Experiments were also performed on some electrodes that had been formed and stored after impregnation but not cycled, with no improvement.

CONCLUSIONS

Dipping electrodes in a solution of cobalt nitrate immediately after impregnation has previously been shown to improve the initial utilization of the electrodes. The effect was studied by comparing the quantity of oxygen evolved during the early cycles for both dipped and undipped electrodes and by examining the impedances and charge-discharge curves of these electrodes. The ohmic resistances of the dipped electrodes were smaller than those of the undipped electrodes, confirming previous studies that the cobalt on the surface produces a more conductive surface film. This reduces the IR losses during charge allowing less oxygen evolution and greater utilization of active material. This cannot account for all of the voltage differences. The kinetic resistances are higher for the undipped material, which is probably due to the higher proportions of inactive material in the undipped electrodes at this early stage of cycling. This would lead to slower rates of diffusion of protons and thus lower rates of reaction at these early stages of cycling. There may be additional effects caused by changes in the oxygen overvoltage with dipping, but the impedance data at high states of charge are not conclusive. The possibility exists that during charging, theresistance of the surface film increases in the undipped electrodes. This would not be observed during these impedance measurements which were done under open-circuit conditions.

Dipping in the cobalt solution to increase the utilization is apparently only effective in the early phases of cycling, since there was no effect on the electrodes that had previously been formed or cycled. Since undipped electrodes eventually improve in utilization so that they are comparable to dipped electrodes, either the surface of the dipped electrode changes with cycling by loss of the very small amount of cobalt on the surface or else the undipped electrode surface increases in conductivity and/or increases the oxygen overvoltage.

REFERENCES

1. Britton, D.L.: Progress in the Development of Lightweight Nickel Electrode. NASA TM-105638, June1992.

2 Britton, D.L.: Characterization and Cycle Tests of Lightweight Nickel Electrodes. NASA TM-102399, Oct. 1989.

3. Britton, D.L.: Progress in the Development of Lightweight Nickel Electrode for Aerospace Applications. NASA TM-103140, March1992.

4. Lee, A.L.; Ferrando, W.A.; and Flight, F.P.: Electrochemical Impregnation of Nickel Composite Electrodes. Naval Surface Weapons Center, NSWC/TR-82-414, 1982.

5. Lee, W.: Optimum Additive Distribution for Quick Activation of Sintered Nickel Composite Electrodes. J. Electrochem. Soc., vol. 132, no. 12, 1985, pp. 2835-2838.

6. Britton, D.L.: Electrochemical Impregnation and Cycle Life of Lightweight Nickel Electrodes for Nickel-Hydrogen Cells. NASA TM-103140, June 1990.

7. Oshitani, M.; Yufu, H.; Takashima, K.; Tsuji, S.; and Matusmaru, Y.: Development of a Pasted Nickel Electrode With High Active Material Utilization. J. Electrochem. Soc., vol. 136, no. 6, 1989, pp. 1590-1593.

8. Haenen, J.; Visscher, W.; and Barendrecht, E.: Oxygen Evolution on Ni-Co Alloys. Electrochim. Acta, vol. 31, no. 12, 1986, pp.1541-1551.

9. Brossard, L.: Cobalt Coatings: Deposition on a Nickel Substrate and Electrocatalytic Activity for Alkaline Water Electrolysis. Materials Chemistry and Physics, vol. 30, 1992, pp. 267-272.

10. Bard, A.J.; and Faulkner, L.R.: Electrochemical Methods. Wiley, New York, 1980.

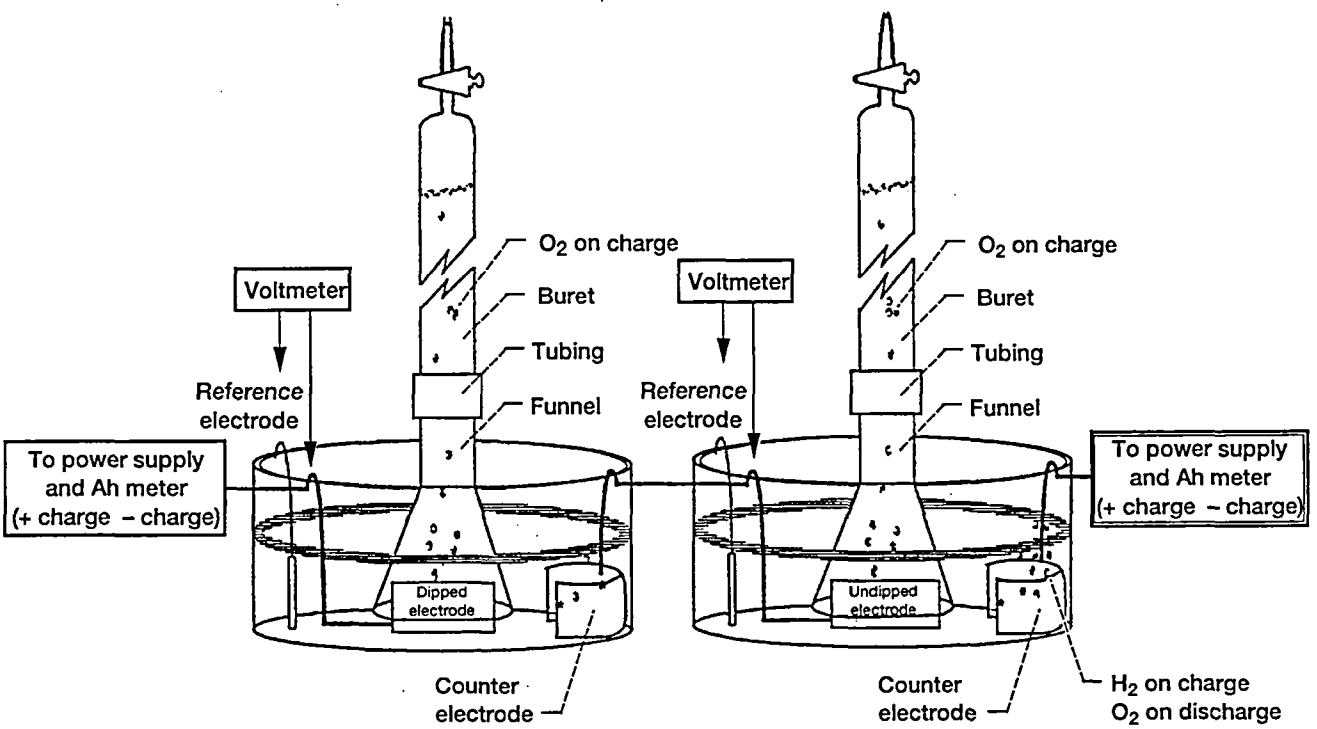

Figure 1.—Setup for experimentally determining amount of oxygen evolved during charge of nickel Fibrex electrodes (counter electrode actually around total circumference of vessel).

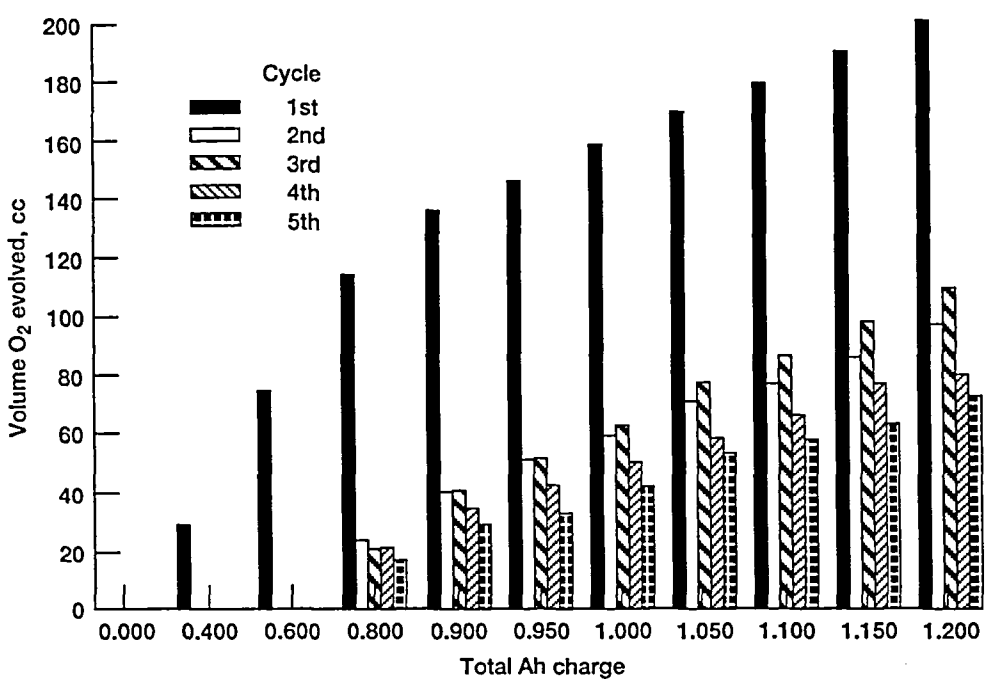

Figure 2.—Results of experiment to determine amount of oxygen evolved during the charge cycles.

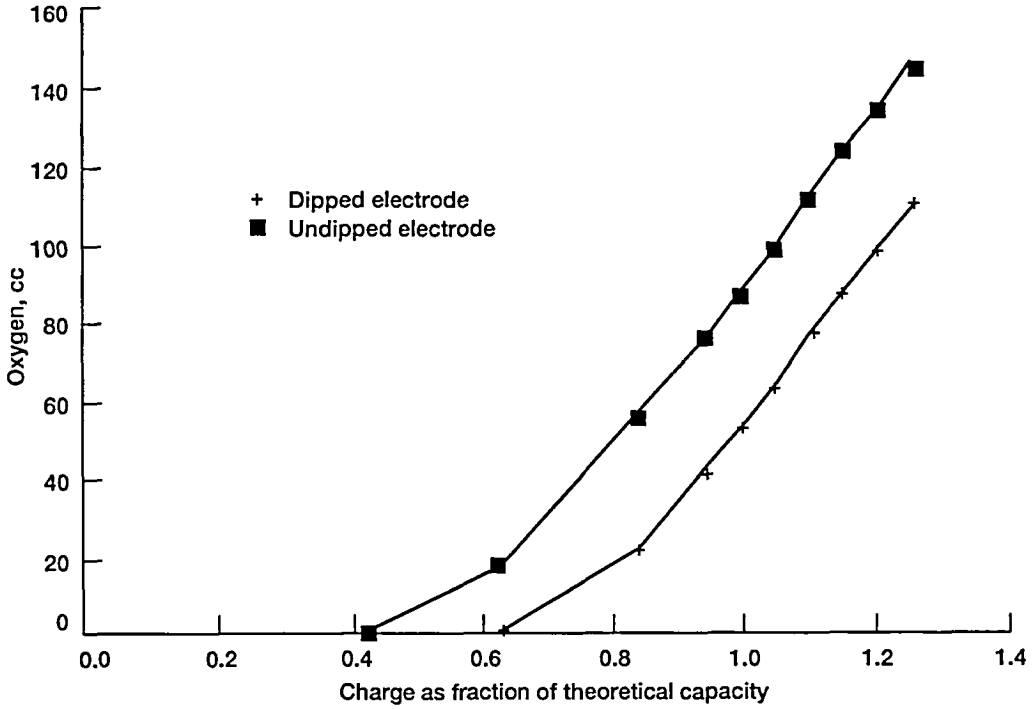

Figure 3.—Oxygen volume differences between dipped versus undipped Fibrex nickel electrodes during third O_2 evolution cycle

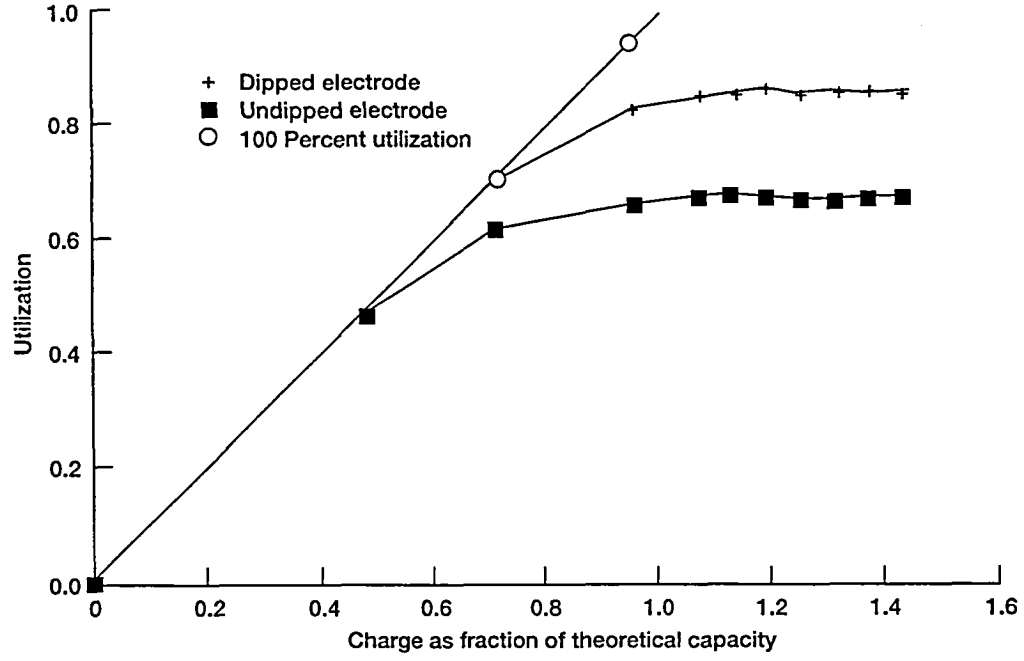

Figure 4.—Utilization of electrode differences between dipped versus undipped Fibrex nickel electrodes during third O_2 cycle.

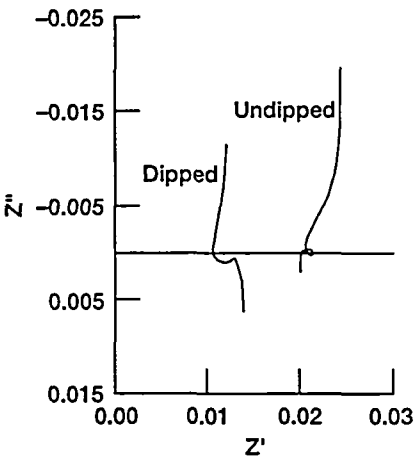

Figure 5.—Complex plane plot performed at 0.440 V versus Hg/HgO.

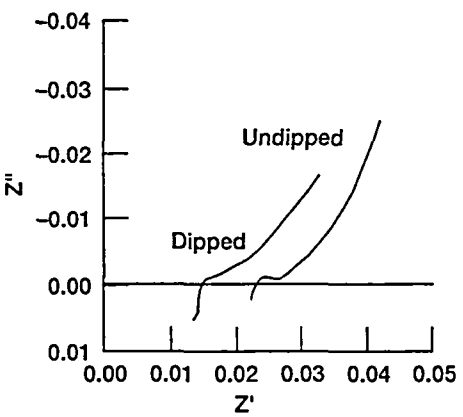

Figure 6.—Complex plane plot performed at 0.290 V versus Hg/HgO.

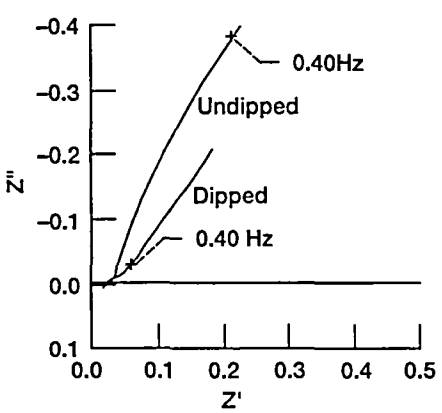

Figure 7.—Complex plane plot performed at 0.220 V versus Hg/HgO.

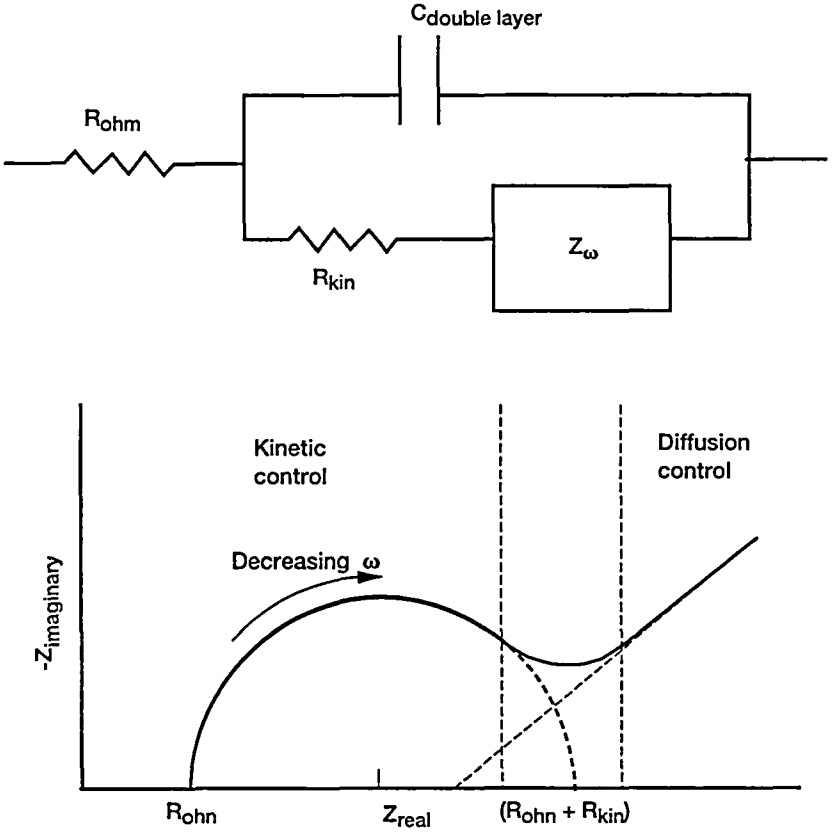

Figure 8.—Simple circuit used to model electrode and idealized complex plane plot for analysis of data (R_{ohn} = resistance; R_{kin} = kinetic resistance, Z = impedance; C = capacitor; ω = frequency).

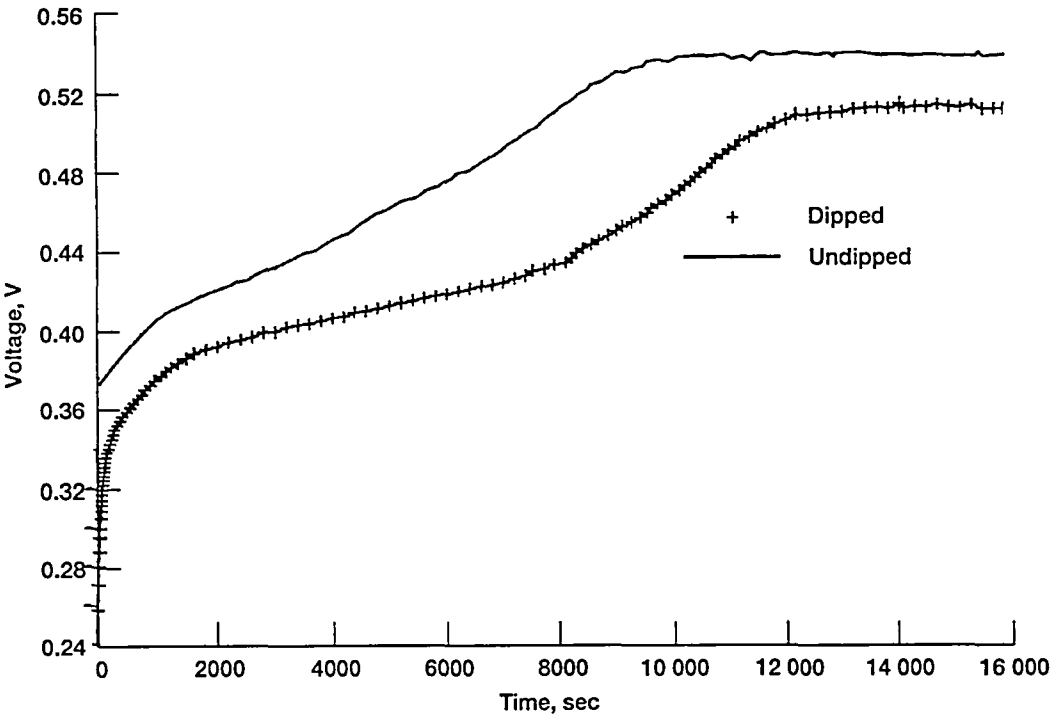

Figure 9.—Charge curves for dipped versus undipped Fibrex nickel electrodes following impedance measurements.

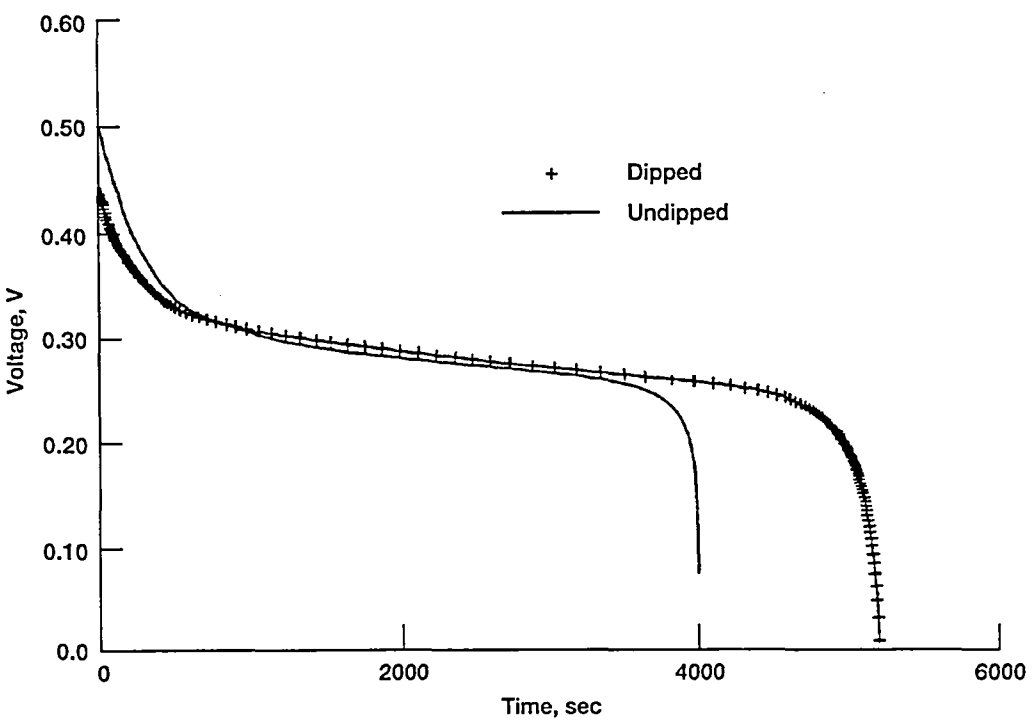

Figure 10.—Discharge curves for dipped versus undipped Fibrex nickel electrodes following impedance measurements.

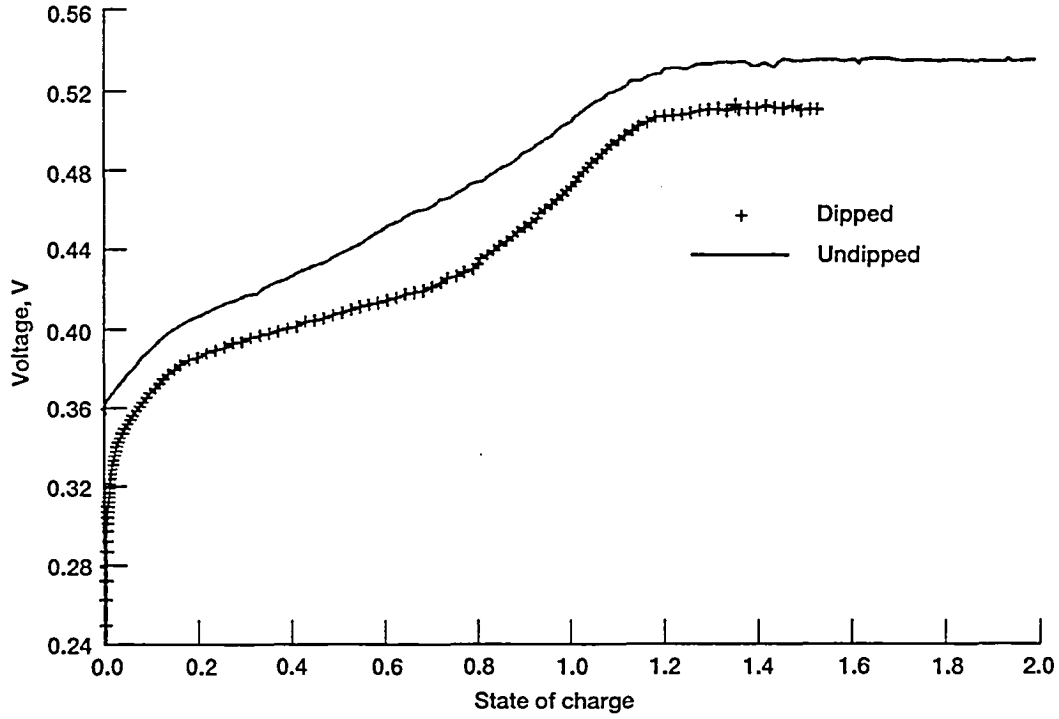

Figure 11.—Charge curves for dipped versus undipped Fibrex nickel electrodes, IR corrected, following impedance measurements.

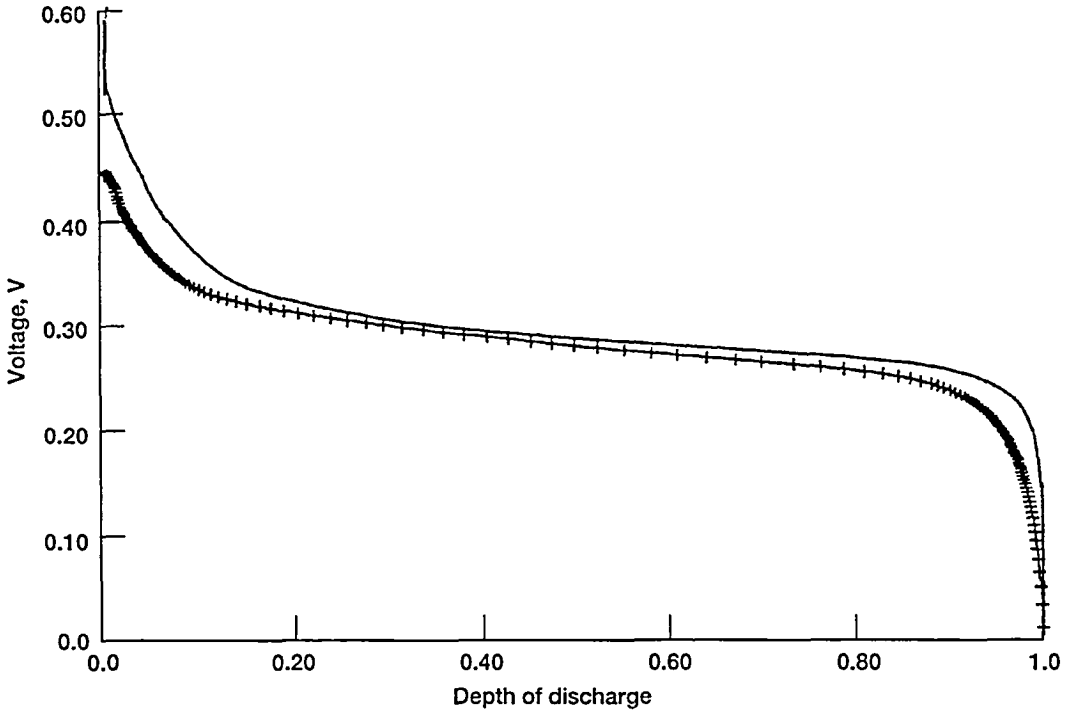

Figure 12.—Discharge curves for dipped versus undipped Fibrex nickel electrodes, IR corrected, following impedance measurements.

REPORT DOCUMENTATION PAGE

Form Approved
OMB No. 0704-0188

1. AGENCY USE ONLY (*Leave blank*)	2. REPORT DATE	3. REPORT TYPE AND DATES COVERED
	August 1995	Technical Memorandum

4. TITLE AND SUBTITLE

Characterization of Cobalt-Dipped Nickel Electrodes With Fibrex Substrates

5. FUNDING NUMBERS

WU-297-55-00

6. AUTHOR(S)

Carolyn A. Youngman and Margaret A. Reid

7. PERFORMING ORGANIZATION NAME(S) AND ADDRESS(ES)

National Aeronautics and Space Administration
Lewis Research Center
Cleveland, Ohio 44135-3191

8. PERFORMING ORGANIZATION REPORT NUMBER

E-9726

9. SPONSORING/MONITORING AGENCY NAME(S) AND ADDRESS(ES)

National Aeronautics and Space Administration
Washington, D.C. 20546-0001

10. SPONSORING/MONITORING AGENCY REPORT NUMBER

NASA TM-106969

11. SUPPLEMENTARY NOTES

Responsible person, Carolyn A. Youngman, organization code 5420, (216) 433-5596.

12a. DISTRIBUTION/AVAILABILITY STATEMENT

Unclassified - Unlimited
Subject Categories 26, 20, and 25

This publication is available from the NASA Center for Aerospace Information, (301) 621-0390.

12b. DISTRIBUTION CODE

13. ABSTRACT (*Maximum 200 words*)

Nickel electrodes using fibrous substrates have poorer initial utilization of the active material than those using conventional nickel sinter substrates. Previous investigators had shown that utilization can be dramatically improved by dipping these electrodes in a cobalt solution immediately after the electrochemical impregnation, before formation and cycling is carried out. The present study looked at the gas evolution behavior of dipped and undipped electrodes, impedance curves, and the charge-discharge curves to try to understand the reasons for the improvement in utilization. Impedance measurements under open circuit conditions indicate that some of the improvement is due to a reduction in the ohmic resistance of the surface layer of the particles, in agreement with earlier work. The charge-discharge curves suggest that there may also be an additional increase in the ohmic resistance of the surface layer of the undipped electrode during charging.

14. SUBJECT TERMS

Batteries; Fibrex nickel electrodes; Utilization; Impedance; Cobalt; Cell life

15. NUMBER OF PAGES

16

16. PRICE CODE

A03

17. SECURITY CLASSIFICATION OF REPORT	18. SECURITY CLASSIFICATION OF THIS PAGE	19. SECURITY CLASSIFICATION OF ABSTRACT	20. LIMITATION OF ABSTRACT
Unclassified	Unclassified	Unclassified	

National Aeronautics and
Space Administration

Lewis Research Center
21000 Brookpark Rd.
Cleveland, OH 44135-3191